ORIGINAL RESEARCH

# Simvastatin-Loaded Nanofibrous Membrane Efficiency on the Repair of Achilles Tendons

Chun-Jui Weng[1–3], Chieh-Tun Liao[2], Ming-Yi Hsu [2,4], Fu-Pang Chang[5], Shih-Jung Liu [1,2]

[1]Department of Orthopedic Surgery, Bone and Joint Research Center, Chang Gung Memorial Hospital at Linkou, Taoyuan, Taiwan; [2]Department of Mechanical Engineering, Chang Gung University, Taoyuan, Taiwan; [3]Department of Orthopaedics, Chang Gung Memorial Hospital at Linkou, Taoyuan, Taiwan; [4]Department of Radiology, Chang Gung Memorial Hospital at Linkou, Taoyuan, Taiwan; [5]Department of Pathology and Laboratory Medicine, Taipei Veterans General Hospital, Taipei, Taiwan

Correspondence: Shih-Jung Liu, Department of Orthopedic Surgery, Bone and Joint Research Center, Chang Gung Memorial Hospital at Linkou and Department of Mechanical Engineering, Chang Gung University, 259, Wen-Hwa 1st Road, Kwei-Shan, Taoyuan, 33302, Taiwan, Tel +886-3-2118166, Fax +886-3-2118558, Email shihjung@mail.cgu.edu.tw

**Introduction:** In this study, simvastatin-incorporated poly(D,L-lactide-co-glycolide) (PLGA) nanofibrous mats were fabricated via electrospinning, and their efficacy in the repair of the Achilles tendon was evaluated.

**Methods:** The morphology of spun nanofibers and the in vitro drug release kinetics were assessed, while the in vivo efficacy in tendon repair was tested using a rat model.

**Results:** Images obtained by scanning electron microscopy revealed that spun nanofibers exhibit a porous structure with a fiber diameter of approximately 350 nm. Fourier-transform infrared spectrometry and differential scanning calorimetry demonstrated successful incorporation of pharmaceutical agents into the PLGA nanofibers. The drug-loaded nanofibrous membranes sustainably discharged high concentrations of simvastatin for >28 days at the target site, and drug concentrations in blood were low. Tendons repaired using simvastatin-eluting nanofibers exhibited superior mechanical strength and animal activities to those repaired without nanofibers or with pure PLGA nanofibers.

**Discussion:** Simvastatin-loaded nanofibers demonstrated effectiveness and sustainable capability for the repair of Achilles tendons. Eventually biodegradable drug-eluting nanofibrous mats may be used in humans for the treatment of tendon ruptures.

**Keywords:** simvastatin, nanofibers, tendon repair, sustainable release

## Introduction

The largest tendon of the human body, the Achilles tendon, is an important structure of the ankle joint. Medical conditions involving the Achilles tendon include Achilles tendinopathy, tendinitis, and tendon rupture.[1] Achilles tendon rupture accounts for approximately 20% of all large tendon ruptures,[2] and leads to a reduction of the level of daily activity. Surgical repair is currently the mainstay treatment for acute Achilles tendon rupture. However, due to the low vascularity of the tendon and surrounding soft tissue,[3] healing of the tendon remains a clinical concern.

Statins, termed hydroxy-methyl-glutaryl coenzyme A reductase inhibitors, are pharmaceutical agents frequently used in the USA.[4] Simvastatin, a member of the statin family, is commonly used in the treatment of hypercholesterolemia to improve the cardiovascular condition of patients. Apart from reducing the levels of cholesterol in blood, statins also possess antioxidant, anti-inflammatory,[5,6] osteogenic,[7–9] angiogenic,[10,11] and immune-modulatory[12,13] functions. Hypercholesterolemia is associated with higher rate of rotator cuff tendon tear and slower regeneration of the interface between tendon and bone. Previous studies showed that simvastatin can facilitate osteoblastic differentiation of bone marrow mesenchymal stem cells and enhance the osteogenesis of human/animal osteoblastic cell lines.[14,15] Furthermore, simvastatin has been shown to promote angiogenesis via up-regulation of gene expression of vascular endothelial growth factor (VEGF) and basic fibroblast growth factor (FGF-2). Either VEGF or FGF-2 has been illustrated to prompt bone morphogenic protein (BMP)-2 expression and excite the differentiation of osteoblast obliquely.[16,17] It was also reported

that local delivery of simvastatin accelerates the healing of critical-sized calvarial defects,[18] due to the combined functions of autogenous osteogenic stem cells and endothelial progenitor cells. Despite the benefits of simvastatin in bone regeneration, systemic administration of high levels of simvastatin may lead to increased risks of unfavorable side effects including rhabdomyolysis and inflammatory myopathies.[19] Superior or comparable bone anabolic effects can be anticipated from lower and sustainable discharge of simvastatin through a local delivery scheme.[15]

While the effect of simvastatin in osteochondral regeneration has been explored, no research has discussed its influence on tendons. Several studies have investigated the effect of statins on the healing of tendon or tendon-bone interface, but reported contradictory results.[20–26] Only few studies have evaluated the effect of statins on the Achilles tendon, and those that did yielded variable results.[24,27,28] Additionally, there is no available research concerning the influence of simvastatin on the healing of acute Achilles tendon rupture.

In this study, a degradable nanofibrous membrane composed of poly(D,L-lactide-co-glycolide) (PLGA) was developed as a drug-delivery vehicle to achieve slow drug release for a prolonged period of time. The aim of this approach was to avoid the occurrence of side effects from the long-term usage of simvastatin and maximize the therapeutic period. The effect of the simvastatin-loaded nanofibrous membrane on the healing process of Achilles tendon rupture after surgical repairment was assessed. The in vitro characteristics/drug release profile of the simvastatin-loaded nanofibrous membrane was investigated, and its in vitro efficacy was evaluated using a rat model. We hypothesized that use of the simvastatin-loaded membrane would improve the biomechanical properties of the Achilles tendon and the post-operative level of animal activity.

# Materials and Methods
## Production of Simvastatin-Eluting Nanofibers
Simvastatin, PLGA (lactide:glycolide 50:50, ester terminated, Mw 24,000–38,000 Da), and hexafluoroisopropanol (HFIP) were purchased from Sigma–Aldrich (St. Louis, MO, USA). Nanofibrous membranes of two different polymer:simvastatin ratios (ie, 1:1 and 2:1) were fabricated through an electrospinning technique. To formulate the 1:1 membranes, simvastatin (700 mg) and PLGA (700 mg) were first mixed with 5 mL of HFIP. Experiments were conducted on a lab-made electrospinning equipment that involves a syringe/needle (needle lumen: 0.42 mm), a grounded sheet, and a power supply. The PLGA/simvastatin mixture was conveyed and electrically spun with a syringe pump at a discharge speed of 1.0 mL/h. The grounded sheet was located 15 cm from the needle tip. The voltage imposed on the polymer mixture was +18 kV. The same protocol was followed for the fabrication of the 2:1 membranes, except that 466 mg of simvastatin and 933 mg of PLGA were mixed with 5 mL of HFIP. All spinning procedures were carried out at ambient temperature (25°C).

PLGA/simvastatin nanofibers were recovered from the grounded sheet post spinning, with a thickness of approximately 150 μm. The electrospun specimens were maintained in a chamber at 40°C for 3 days to vaporize the residual solvents.

## Observation Using a Scanning Electron Microscope (SEM)
An SEM (JSM–7500F; Joel, Tokyo, Japan) was employed to examine the simvastatin-loaded nanofibers. One hundred arbitrarily selected fibers were evaluated from the microphotos captured by the SEM to determine the size distribution of spun nanofibers.

## Wetting Angle Measurement
The wetting angles of pure PLGA and simvastatin-loaded nanofibers (both 1:1 and 2:1 polymer:drug ratios) were evaluated. Distilled water was gently dribbled on the surface of nanofibrous samples (10 mm × 10 mm) and monitored using a video camera (Imaging Source, Taipei, Taiwan) (n=3).

## Fourier Transform Infrared (FTIR) Spectroscopy
FTIR spectroscopy analysis was conducted using a Model Bruker Tensor 27 spectrometer (San Jose, CA, USA). The resolution was 4 cm$^{-1}$ in absorption mode, using 32 scans in total. The nanofibrous specimens were compressed into potassium bromide discs and analyzed within the range of 500–4000 cm$^{-1}$.

## Differential Scanning Calorimetry (DSC)

Pure PLGA, simvastatin, and simvastatin-loaded PLGA nanofibrous mats were analyzed using a TA-DSC25 DSC (TA Instruments, New Castle, DE, USA). The scanning temperature ranged from 30 to 200°C, with a heating speed of 10°C/min.

## In vitro Discharge Behavior of Simvastatin

The discharge behavior of simvastatin from the PLGA nanofibrous mats was assessed using an in vitro elution scheme. Electrospun specimens (10 mm × 10 mm) were submerged in 1 mL of phosphate-buffered saline inside a glass tube (n=3). Following incubation for 24 h at 37°C, the buffer was replaced by fresh phosphate buffered saline daily for 30 days. The concentration of simvastatin in the mixture was subsequently estimated by high-performance liquid chromatography (L-2200R multi-solvent delivery system; Hitachi, Tokyo, Japan).

## Animal-Related Procedures

Sixty Sprague–Dawley rats (weight: 250±25 g) were included in the animal study. All animal experiments and related procedures were performed by a veterinarian according to the ordinances of the Department of Health and Welfare, Taiwan. The animal experiments were also approved by the Chang Gung University Institutional Animal Care and Use Committee (CGU108-121).

Prior to Surgery, the rats were placed inside a transparent box (40 cm × 20 cm × 28 cm) and anesthetized through administration of vaporized isoflurane. Subsequently, each rat was placed on a sterilized sheet, and its head was covered with a mask filled with continuously administered vaporized isoflurane throughout the surgery. A skin incision (3 cm) over the postero-medial side of the left leg was made longitudinally using a No. 15 blade. The soft tissue was dissected with the blade to expose the Achilles tendon from the distal insertion to the proximal muscle part (Figure 1A). Following circumferential dissection, the Achilles tendon was transected transversely and repaired with 5-0 Dexon (Johnson & Johnson, USA) interrupt suture (Figure 1B). In the control group, the wound was closed with 3-0 Nylon following repair of the Achilles tendon. In the PLGA membrane group, the repaired tendon of rats was wrapped with pure PLGA membrane. In the drug-eluting membrane group, the repaired tendon was wrapped with simvastatin-loaded PLGA membrane (Figure 1C).

Forty-five rats were divided into three groups and underwent: 1) tendon repair (control group); 2) tendon repair along with implantation of pure PLGA membrane (PLGA membrane group); or 3) tendon repair along with implantation of simvastatin-loaded nanofibrous membrane (drug-eluting membrane group). Each group consisted of 15 rats and was divided into three sub-groups (five rats per sub-group). In addition to the three groups of rats that received tendon repair, another five rats did not undergo surgery (normal tendon group).

## In vivo Drug Release

The in vivo systemic drug concentrations were assessed by collecting blood samples with syringes (heart puncture) from the rats. The local drug concentrations were evaluated by tissue sampling near the implantation site. The drug concentrations, both systemically and locally, were assayed by high-performance liquid chromatography on postoperative days 1, 3, 7, 14, and 28 (n=5).

## Post-Surgery Activity

After surgery, each rat was maintained in an activity behavior cage[29] to observe the degree of postoperative activity. The cage was equipped with nine photoelectric sensors on top of nine symmetric square regions. As the rat moved from one region to another, the corresponding sensor at the "arriving" region was triggered. The total number of times the sensors were triggered over a period of 7 days was recorded. The activities of rats in the four aforementioned groups were assessed (n=5).

## Biomechanical Strength of Tendons

The rats were first euthanized by intravenous injection of lidocaine (10 mL) at 1, 2, and 4 weeks post operation. The right Achilles tendons and the left healthy tendons of rats were retrieved at 1, 2, and 4 weeks for biomechanical testing (n=5).
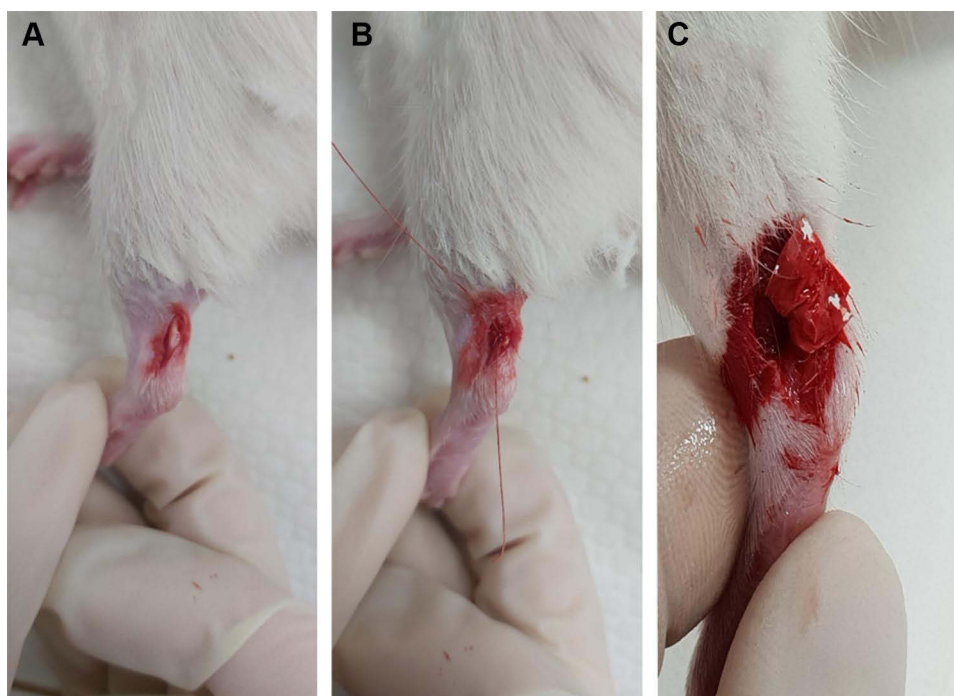
**Figure 1** (**A**) Dissection of Achilles tendon. (**B**) Repair of the tendon with suture. (**C**) Wrapping of simvastatin-loaded membrane onto repaired tendon.

Experiments were conducted on a tensile tester (Lloyd, Ametek, USA). The pull speed for the tests was 60 mm/min. The tensile strengths and elongations of the tendons were recorded.

## Histological Analysis

Following euthanasia of the rats and retrieval of tendons, specimens were fixed in 10% formalin and embedded in paraffin. Next, each specimen was sliced at the frontal end (thickness: 4 μm). Two different staining methods were used: hematoxylin and eosin (H&E), and trichrome staining. H&E staining was used for the assessment of white blood cell accumulation, which represents the degree of inflammation. Trichrome staining was used to evaluate the amount and differentiation of tenocytes into mature tendon cells. Sectioned slides were assessed by an independent pathology doctor, blinded to the control and experiment groups. Collagenization, collagen construction, and the degree of revascularization were also observed and recorded.

## Statistical Analysis

All data are presented as mean ± standard deviation and evaluated via the paired $t$-test for statistical evaluation between different two-group combination, using SPSS software (Version 12.0; SPSS, Chicago, IL, USA). For all analyses, a p-value <0.05 denoted statistically significant difference.

## Results
### Characterization of Spun Simvastatin-Loaded Nanofibers

Simvastatin-loaded nanofibrous membranes were fabricated using the electrospinning method. Figure 2A illustrates the SEM image and the fiber size distribution of the spun polymer:drug 1:1 nanofibers, and Figure 2B displays those of the 2:1 nanofibers. The calculated diameter distributions of the 1:1 and 2:1 spun nanofibers were 330.6±137.3 nm and 390.3 ±134.4 nm (p>0.05), respectively.

Figure 3 shows the wetting angles of pure PLGA, 1:1 PLGA-to-drug-ratio, and 2:1 PLGA-to-drug-ratio nanofibers, which were estimated to be 127.4°, 27.6°, and 88.4°, respectively. Although the pure PLGA nanofibers exhibited
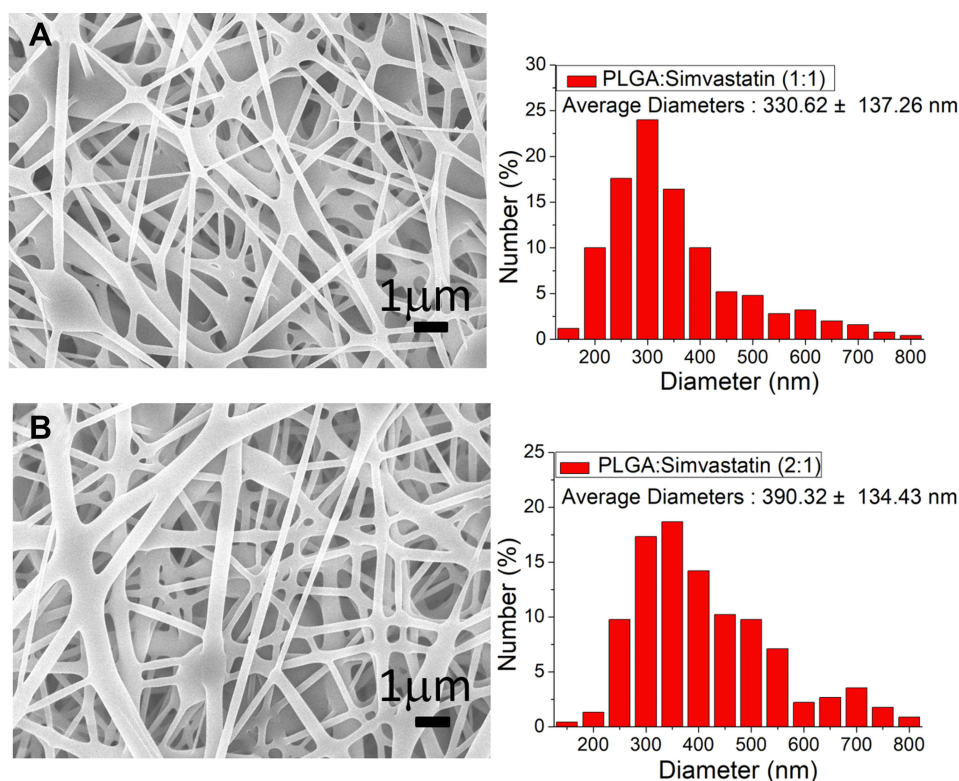
**Figure 2** SEM image and fiber size distribution of nanofibers with a PLGA:simvastatin ratio of (**A**) 1:1 and (**B**) 2:1.

hydrophobic characteristics, the water-soluble simvastatin in the drug-loaded PLGA samples markedly improved the hydrophilicity of the electrospun fibrous mats.

Figure 4 shows the results of the FTIR spectroscopy assay for the pure PLGA and simvastatin-loaded PLGA nanofibers. The enhanced peak at 3550 cm$^{-1}$ was derived from the O-H bond of the added drug. The new vibration near 2950 cm$^{-1}$ was caused by the C=C of simvastatin.[30] In addition, the significantly enhanced vibrations observed at 870 cm$^{-1}$ and 1267 cm$^{-1}$ could be attributed to the C-H bonds of the drug,[31] while the peak noted at 1390 cm$^{-1}$ was due to the CH$_2$ bond of added simvastatin. These results demonstrated that simvastatin had been successfully incorporated into the PLGA nanofibrous mats.

The thermal characteristics of pure PLGA, simvastatin, and simvastatin-loaded PLGA nanofibers were also investigated. The endothermal peak of simvastatin at 138°C (Figure 5) diminished after its embedding into the PLGA mat, further confirming the successful incorporation of simvastatin in the PLGA nanofibrous membranes.

## In vitro and in vivo Releases

Figure 6 illustrates the daily and accumulated release behaviors of simvastatin in vitro from the nanofibrous mats. The release pattern exhibited a biphasic discharge, ie, a burst discharge at 1 day and a progressive diminishing and steady drug release thereafter. Additionally, the simvastatin-incorporated nanofibers offered extended discharge of simvastatin in vitro for 30 days.

Figure 7 illustrates the in vivo release behaviors of simvastatin in blood and tissue. The drug levels at the tendon remained high for 28 days, whereas the systemic concentration of simvastatin was low.

## Biomechanical Properties

At week 1 (Figure 8A), the maximum strength recorded in the simvastatin-loaded membrane group (12.43±2.36 N) was significantly higher than that measured for the pure PLGA membrane group (2.59±1.89 N) (p=0.167) as well as higher
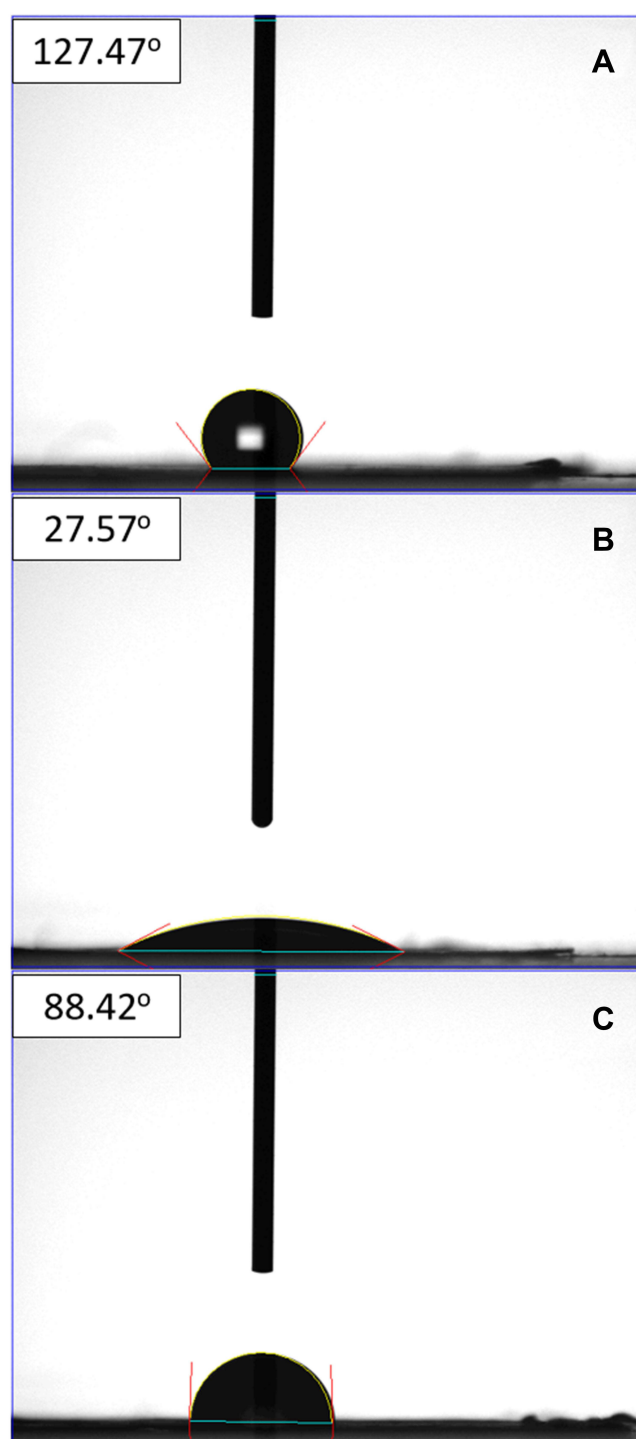
**Figure 3** Wetting angles of (**A**) pure PLGA membrane, (**B**) PLGA:simvastatin 1:1 membrane, and (**C**) PLGA:simvastatin 2:1 membrane.

than that for control group (3.06±4.79 N) (p=0.09). The tendons treated using the simvastatin-loaded membrane also exhibited comparable strength to that of normal tendons (14.96±2.76 N) (p=0.262).

At 2 weeks (Figure 8B), the tendon strengths of rats in both the control and pure PLGA membrane groups were increased (4.95±1.70 N and 9.48±1.65 N, respectively); however, they remained lower than those noted in the simvastatin-loaded membrane group (16.47±8.09 N) (control vs simvastatin-loaded membrane: p=0.063; pure PLGA
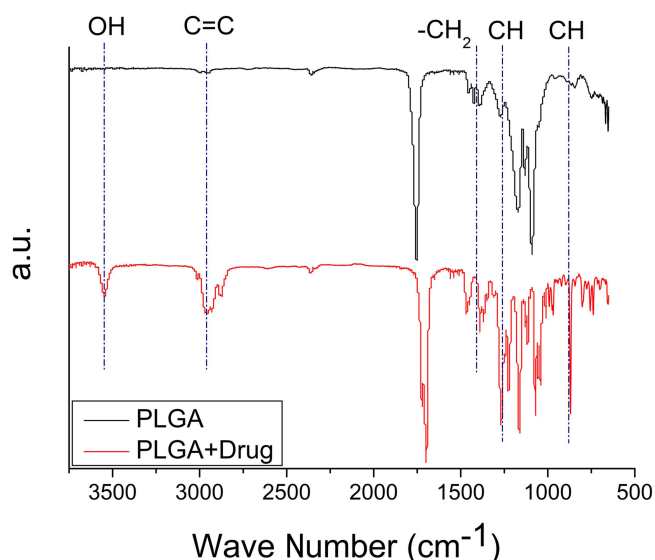
**Figure 4** FTIR spectra of PLGA and simvastatin-loaded PLGA nanofibers.
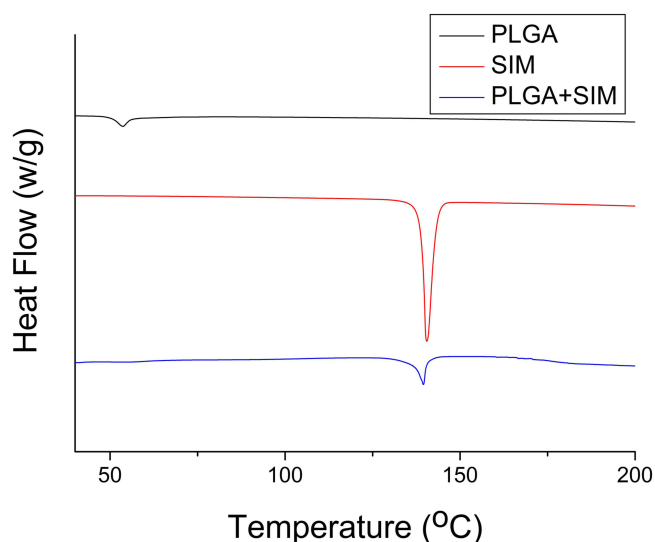


**Figure 5** Thermal behaviors of PLGA, simvastatin, and simvastatin-loaded PLGA nanofibers.

vs simvastatin-loaded membrane: p=0.135). Interestingly, the simvastatin-loaded membrane group exhibited higher tendon strength than even the normal tendon group (11.01±1.06 N) (p=0.182).

At 4 weeks (Figure 8C), the maximum load of the drug-eluting membrane group (13.20±3.70 N) was lower than that of the normal tendon group (26.14±4.13 N) (p=0.0079). Nevertheless, it remained higher than those of the pure PLGA membrane group (9.22±2.35 N) (p=0.10) and control group (11.82±3.09 N) (p=0.323). These findings demonstrate the effectiveness of simvastatin-loaded nanofibers in the treatment of Achilles tendon rupture.

## Animal Activity

An activity cage was utilized to assess rat activity after the operation. The total trigger times for distinct groups are illustrated in Figure 9. The trigger counts for the control, simvastatin-eluting nanofibers, pure PLGA nanofibers, and surgery-only groups were 10,508±1336, 8725±2096, 5384±1913 and 5476±173, respectively. The surgery-only and pure PLGA groups showed significantly lower levels of activity compared with the control group (p<0.01). However, there was no significant difference between the simvastatin-eluting nanofibers and control groups (p>0.05). This indicates that
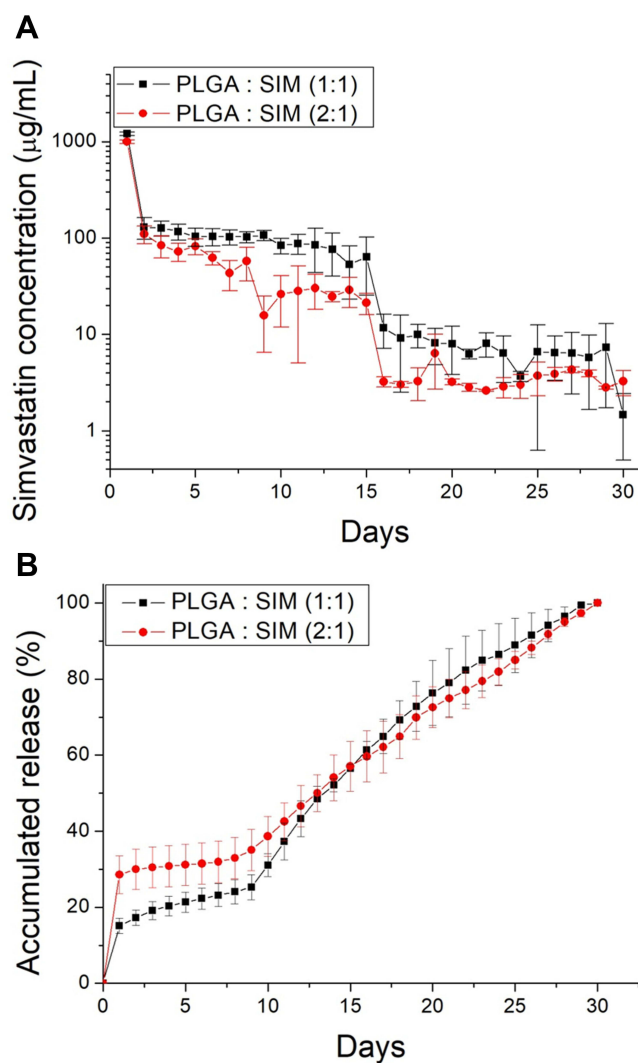
**Figure 6** In vitro (**A**) daily and (**B**) cumulative release of simvastatin from PLGA nanofibers.
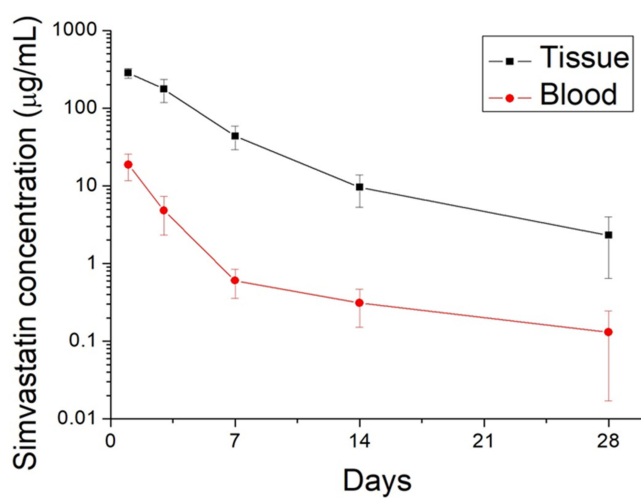


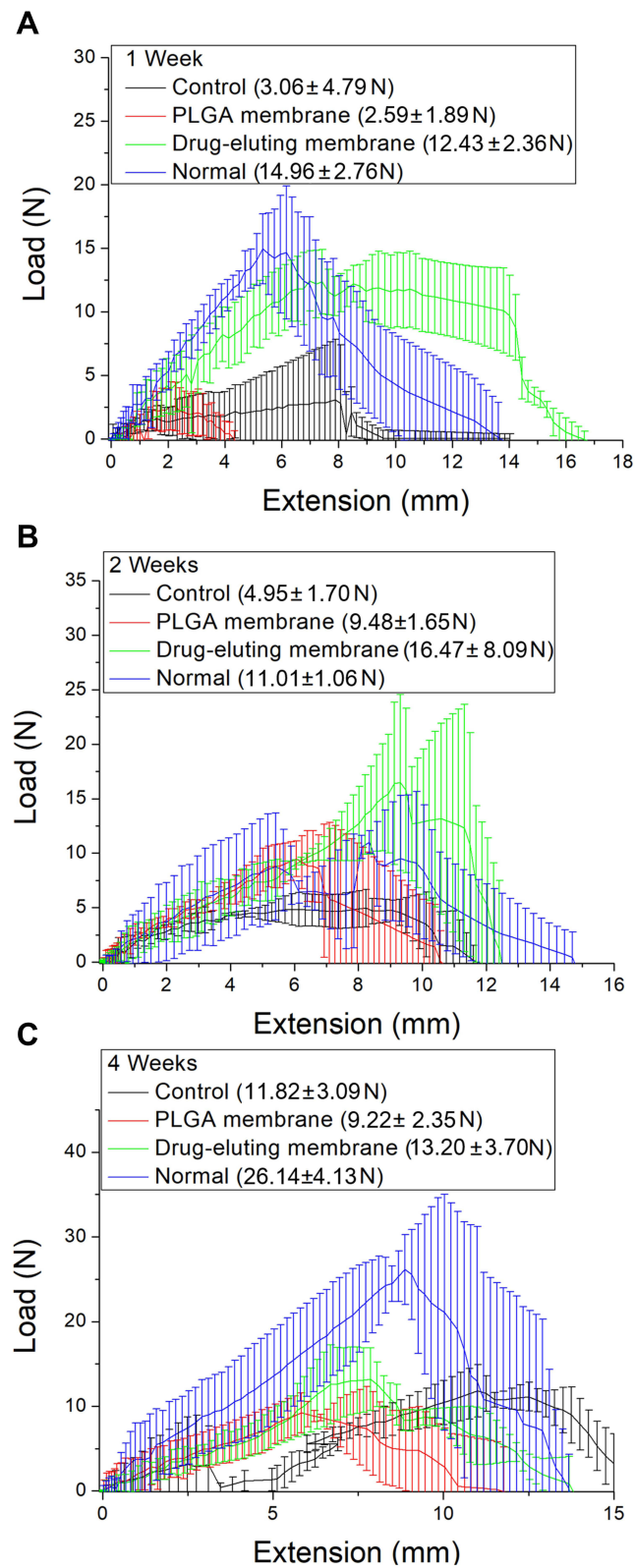**Figure 7** In vivo release of simvastatin-incorporated nanofibers.

**Figure 8** Mechanical strength of retrieved tendons at (**A**) 1, (**B**) 2, and (**C**) 4 weeks post operation.

the rats undergoing Achilles tendon repair with simvastatin-incorporated PLGA nanofibrous mats exhibited a comparable degree of activity to rats that did not undergo surgery. Moreover, these rats showed higher activity levels than those who underwent surgery only (without nanofibrous membrane) or were treated with a pure PLGA membrane. These experimental results confirmed the efficacy of drug-eluting nanofibers in the treatment of tendon rupture.

## Histological Analysis Results

The images obtained after H&E staining did not show significant differences in white blood cell infiltration versus control at any of the time points assessed. In other words, PLGA membrane alone and simvastatin-loaded membrane did not induce a more severe inflammatory response compared with that observed in the control group. However, based on the results of trichrome staining, the largest area of dense collagen fibers was noted in the drug-eluting membrane group at 2 weeks, followed by the control group. There were almost no dense collagen fibers observed in the PLGA group (Figure 10A–C). H&E staining yielded similar results at 2 weeks. There was no difference in the area of dense collagen fibers between all groups at 1 and 4 weeks (Figure 10D–F). The results of the histological analysis showed better tendon healing for rats in the drug-eluting membrane group compared with the other groups at 2 weeks; however, this difference was not observed at 1 or 4 weeks.

## Discussion

Achilles tendon rupture principally affect sports activity after injury, since this tendon is the largest and strongest of the human body.[1] In most circumstances, Achilles tendon rupture occurs at the mid-substance of the tendon. Therefore, primary repair between both sides of the tendon has been the main treatment choice at the acute stage.[2,6]

Statins have been used in the treatment of hyperlipidemia for a long period of time.[4,32] Simvastatin, acting as a hydroxy-methyl-glutaryl coenzyme A reductase inhibitor, is one of the most widely used medications worldwide. It has been demonstrated that simvastatin decreases the risk of cardiovascular disease. Rare adverse effects associated with
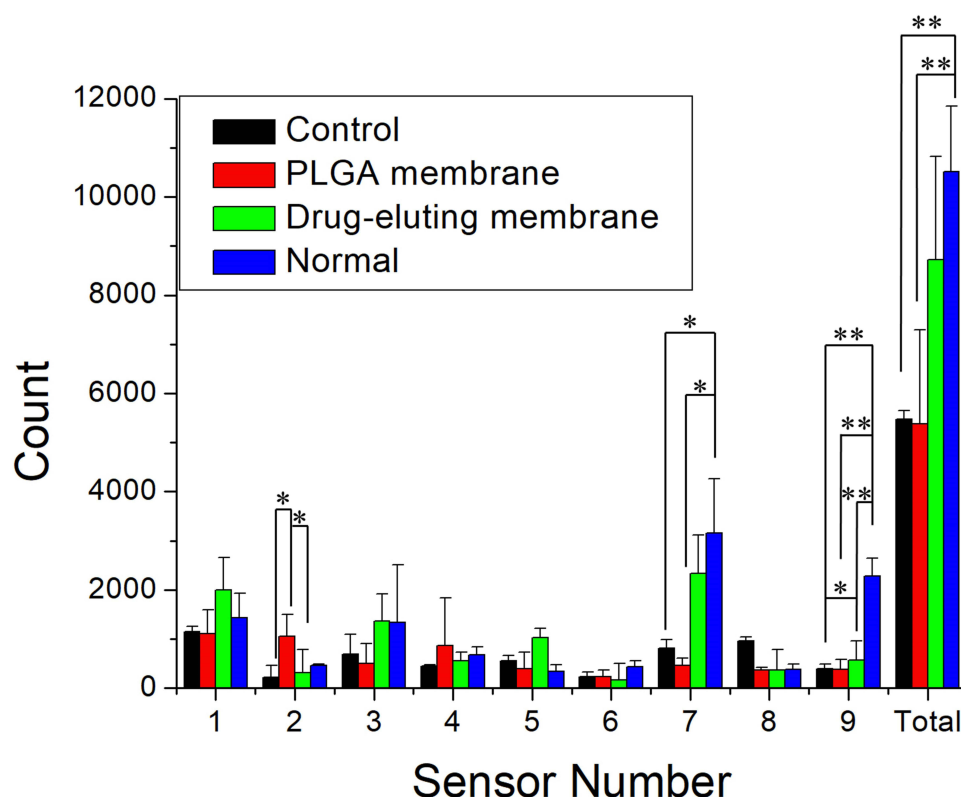
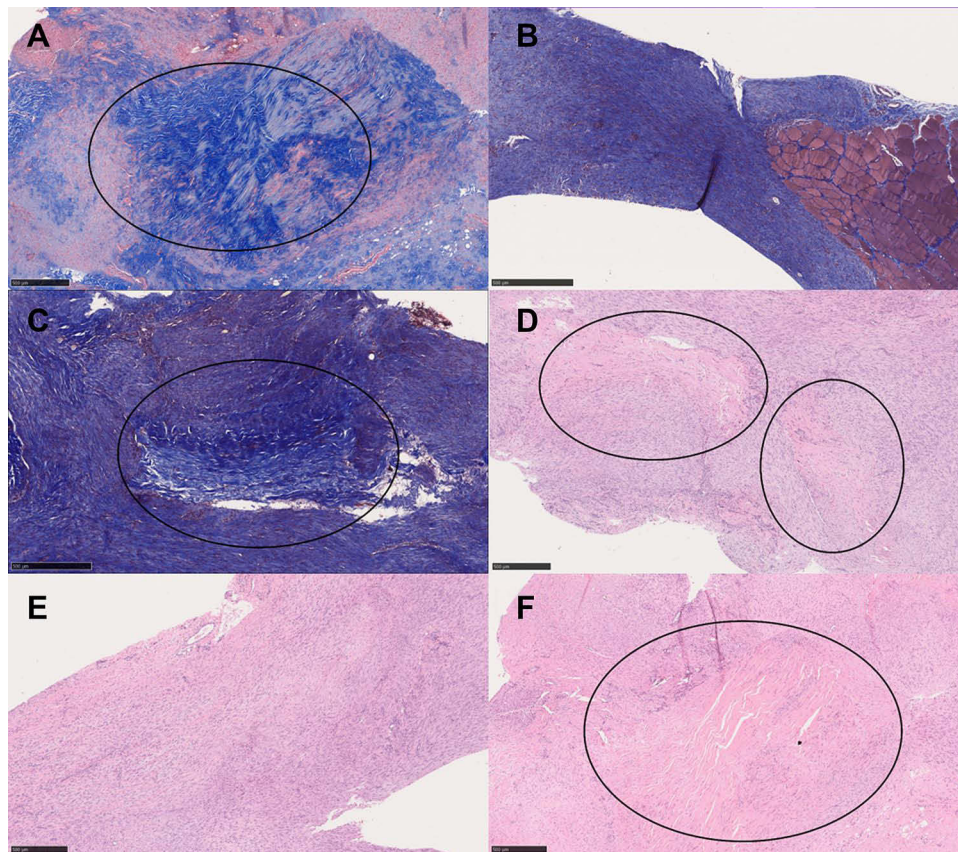**Figure 9** Animal activity counts of rats in various groups. (*p<0.05; **p<0.01).

**Figure 10** Histology results at 2 weeks with trichrome staining (**A–C**) and H&E staining (**D–F**). (**A**) Trichrome staining of the control group. (**B**) Trichrome staining of the PLGA membrane group. (**C**) Trichrome staining of the drug-eluting membrane group. (**D**) H&E staining of the control group. (**E**) H&E staining of the PLGA membrane group. (**F**) H&E staining of the drug-eluting membrane group. The black circle shows the area with dense collagen fiber, which was largest in the drug-eluting membrane group. Scale bar: 500 μm.

simvastatin include myopathy, rhabdomyolysis, and increase in the levels of hepatic transaminase.[32] Statins possess anti-inflammatory, anti-oxidative, and angiogenic functions.[33,34] Moreover, statins exert controversial effects on the tendon and bone. Animal studies revealed that simvastatin can enhance the osteogenic process in bone defects.[35,36] It can also improve healing of the tendon-bone interface of anterior cruciate ligament reconstruction in rabbits.[22] However, other studies concerning the effect of statins on the tendon showed contradictory results.[21,37] For example, in patients with hyperlipidemia, it has been suggested that statins may have a protective effect against tendinopathies;[38–40] however, other investigations proposed that statins may increase the possibility of tendinopathy or rupture.[41–43]

Several studies have shown positive effects of simvastatin on the tendon. Tucker et al[23] studied the effect of simvastatin on the supraspinatus tendon in hypercholesterolemic rats. Simvastatin was administered orally to rats for 3 months, after which the animals were sacrificed to conduct biomechanical and histological evaluations. The investigators found improved mechanical and histological properties in the simvastatin-treated group. Davis et al[21] performed experiments on rats receiving simvastatin through oral gavage after undergoing tenotomy of the supraspinatus tendon. They concluded that simvastatin partially protects the supraspinatus tendon from weakness and substantially from fibrosis. Jeong et al[27] injected microspheres loaded with simvastatin into rats with Achilles tendinitis. They concluded that simvastatin-loaded porous microspheres increase the collagen content, stiffness, and tensile strength of the tendon, and may eventually improve tendon healing.

However, a few studies have suggested a minimal or even negative effect of statins on tendon healing. Esenkaya et al[37] orally administered atorvastatin to rabbits with a surgically ruptured and repaired Achilles tendon for 6 weeks. They found a statistically significant difference in collagen production, but no difference in fibroblastic activity. Differences in revascularization, collagenization, and inflammatory cell infiltration were also observed histologically,

but did not reach statistical significance. Deren et al[26] showed that locally used simvastatin-loaded polylactic acid membrane or oral administration of simvastatin were not beneficial to healing after rotator cuff repair. Eliasson et al[25] conducted an in vitro cell culture experiment, showing that simvastatin and atorvastatin decreased the cell proliferation and mechanical strength of the tendon construct.

In the present study, a simvastatin-incorporated PLGA nanofibrous membrane was developed for the repair of Achilles tendons. PLGA is one of the most attractive polymers used in the fabrication of implants for various medical applications.[44,45] This material is biocompatible and biodegradable, displays a wide range of degradation times, and possesses tailorable mechanical properties; importantly, it is approved by the US Food and Drug Administration. Furthermore, PLGA has been widely investigated as a vehicle for the delivery of pharmaceuticals, proteins, and other biomolecules. Electrospinning can be used to prepare nanoscale continuous fibers.[46] This technique is also capable of producing distinct fiber assemblies, such as nonwoven and aligned fibrous meshes, patterned fiber mats, random three-dimensional structures, sub-micron spring, and convoluted fibers.[47]

In general, the release of pharmaceuticals from a drug-loaded degradable nanocarrier consists of three different stages: a preliminary burst, diffusion-controlled discharge, and degradation-governed elution.[48] Although the majority of pharmaceuticals are embedded inside the matrix of PLGA nanofibers, following the electrospinning procedure, a limited amount of drug may be present in the exterior of the fibers, leading to a burst release. Thereafter, the pharmaceutical-release patterns are simultaneously governed by diffusion and polymeric material degradation. A steadily diminishing release of analgesics was thus observed. Overall, the PLGA nanofibrous membranes were able to discharge high concentrations of simvastatin at the target location for >28 days.

The morphology of the extracellular matrix (ECM) has been widely studied in multiple tissues, including bone, fibrocartilage, Achilles tendon, and ligament. Despite the great diversity among different tissues, the microstructure and composition of the ECM play vital roles in the retention of physiological homeostasis and progression of pathological conditions.[49] An ideal scaffold for tendon repair should imitate the native ECM and be able to support cell adhesion, proliferation, and maturation. Electrospun nanofibrous membranes possess the potential to resemble the ECM and are adjustable to retain suitable porosity, gas permeability, and mechanical integrity. In turn, these characteristics support the capability of such membranes for tissue Engineering.[50] The large surface area and porous structure of spun nanofibrous mats also permit promotion of cell functionality after the embedment of multiple factors. Furthermore, the electrospun nanofibers can be enriched through various surface modification strategies.[51]

The drug-loaded scaffold developed in this work comprises a diverse interwoven nanofibrous structure that mimics the architecture of the ECM, and provides a sustainable release of simvastatin for >28 days. In addition, the drug-eluting nanofibrous membrane possesses good flexibility. The size and geometry of the membrane can also be easily tailored using scissors or a cutter. Implantation of the membrane is based on the conventional tendon-repair procedure. By adopting similar implantation schemes as those utilized in current clinical practice, the learning curve can be reduced, established clinical principles and experience are used, and clinical acceptance is supported. This provides advantages in terms of the implantation of drug-eluting nanofibers.

Notwithstanding these encouraging preliminary findings, the study was subject to limitations. Firstly, the number of animals included in the experiments was relatively low. Secondly, the period of activity surveyed was limited. Finally, the correlation between our findings and tendon healing in humans remains unknown and warrants further investigation.

## Conclusions

A simvastatin-incorporated PLGA nanofibrous mat was successfully developed via electrospinning for the repair of Achilles tendon. Electrospun nanofibers exhibited a porous structure with a fiber diameter of approximately 350 nm, mimicking the microstructure of the ECM. The drug-loaded nanofibrous membranes sustainably discharged high concentrations of simvastatin for >28 days at the target area, whereas the drug concentrations in blood remained low. Tendons repaired with the simvastatin-eluting nanofibers exhibited superior mechanical strength and enabled higher post-operational animal activities versus those repaired without nanofibers or with pure PLGA nanofibers. Simvastatin-loaded nanofibers demonstrated effectiveness and sustainable capability for the treatment of Achilles tendons.

## Acknowledgments

## Disclosure

The authors declare no conflicts of interest in this work.

## References

1. Jarvinen TA, Kannus P, Maffulli N, Khan KM. Achilles tendon disorders: etiology and epidemiology. *Foot Ankle Clin*. 2005;10(2):255–266. doi:10.1016/j.fcl.2005.01.013
2. Gillies H, Chalmers J. The management of fresh ruptures of the tendo achillis. *J Bone Joint Surg Am*. 1970;52(2):337–343. doi:10.2106/00004623-197052020-00015
3. Yepes H, Tang M, Geddes C, Glazebrook M, Morris SF, Stanish WD. Digital vascular mapping of the integument about the Achilles tendon. *J Bone Joint Surg Am*. 2010;92(5):1215–1220. doi:10.2106/JBJS.I.00743
4. Parker BA, Thompson PD. Effect of statins on skeletal muscle: exercise, myopathy, and muscle outcomes. *Exerc Sport Sci Rev*. 2012;40(4):188–194. doi:10.1097/JES.0b013e31826c169e
5. Albert MA, Danielson E, Rifai N, Ridker PM; Prince Investigators and PRINCE Investigators. Effect of statin therapy on C-reactive protein levels: the pravastatin inflammation/CRP evaluation (PRINCE): a randomized trial and cohort study. *JAMA*. 2001;286(1):64–70. doi:10.1001/jama.286.1.64
6. Okura H, Asawa K, Kubo T, et al. Impact of statin therapy on systemic inflammation, left ventricular systolic and diastolic function and prognosis in low risk ischemic heart disease patients without history of congestive heart failure. *Intern Med*. 2007;46(17):1337–1343. doi:10.2169/internalmedicine.46.0021
7. Fukui T, Ii M, Shoji T, et al. Therapeutic effect of local administration of low-dose simvastatin-conjugated gelatin hydrogel for fracture healing. *J Bone Miner Res*. 2012;27(5):1118–1131. doi:10.1002/jbmr.1558
8. Tanigo T, Takaoka R, Tabata Y. Sustained release of water-insoluble simvastatin from biodegradable hydrogel augments bone regeneration. *J Control Release*. 2010;143(2):201–206. doi:10.1016/j.jconrel.2009.12.027
9. Skoglund B, Aspenberg P. Locally applied Simvastatin improves fracture healing in mice. *BMC Musculoskelet Disord*. 2007;8:98. doi:10.1186/1471-2474-8-98
10. Matsumura M, Fukuda N, Kobayashi N, et al. Effects of atorvastatin on angiogenesis in hindlimb ischemia and endothelial progenitor cell formation in rats. *J Atheroscler Thromb*. 2009;16(4):319–326. doi:10.5551/jat.no026
11. Bitto A, Minutoli L, Altavilla D, et al. Simvastatin enhances VEGF production and ameliorates impaired wound healing in experimental diabetes. *Pharmacol Res*. 2008;57(2):159–169. doi:10.1016/j.phrs.2008.01.005
12. Tsai WC, Yu TY, Lin LP, Cheng ML, Chen CL, Pang JH. Prevention of simvastatin-induced inhibition of tendon cell proliferation and cell cycle progression by geranylgeranyl pyrophosphate. *Toxicol Sci*. 2016;149(2):326–334. doi:10.1093/toxsci/kfv239
13. McFarland AJ, Davey AK, Anoopkumar-Dukie S. Statins reduce lipopolysaccharide-induced cytokine and inflammatory mediator release in an in vitro model of microglial-like cells. *Mediators Inflamm*. 2017;2017:2582745. doi:10.1155/2017/2582745
14. Ruiz-Gaspa S, Nogues X, Enjuanes A, et al. Simvastatin and atorvastatin enhance gene expression of collagen type 1 and osteocalcin in primary human osteoblasts and MG-63 cultures. *J Cell Biochem*. 2007;101(6):1430–1438. doi:10.1002/jcb.21259
15. Yu WL, Sun TW, Qi C, et al. Enhanced osteogenesis and angiogenesis by mesoporous hydroxyapatite microspheres-derived simvastatin sustained release system for superior bone regeneration. *Sci Rep*. 2017;7:44129. doi:10.1038/srep44129
16. Maeda T, Matsunuma A, Kurahashi I, Yanagawa T, Yoshida H, Horiuchi N. Induction of osteoblast differentiation indices by statins in MC3T3-E1 cells. *J Cell Biochem*. 2004;92(3):458–471. doi:10.1002/jcb.20074
17. Wong RW, Rabie AB. Early healing pattern of statin-induced osteogenesis. *Br J Oral Maxillofac Surg*. 2005;43(1):46–50. doi:10.1016/j.bjoms.2004.08.014
18. Yueyi C, Xiaoguang H, Jingying W, et al. Calvarial defect healing by recruitment of autogenous osteogenic stem cells using locally applied simvastatin. *Biomaterials*. 2013;34(37):9373–9380. doi:10.1016/j.biomaterials.2013.08.060
19. Oryan A, Kamali A, Moshiri A. Potential mechanisms and applications of statins on osteogenesis: current modalities, conflicts and future directions. *J Control Release*. 2015;215:12–24. doi:10.1016/j.jconrel.2015.07.022
20. Zhang Y, Yu J, Zhang J, Hua Y. Simvastatin with PRP promotes chondrogenesis of bone marrow stem cells in vitro and wounded rat achilles tendon-bone interface healing in vivo. *Am J Sports Med*. 2019;47(3):729–739. doi:10.1177/0363546518819108
21. Davis ME, Korn MA, Gumucio JP, et al. Simvastatin reduces fibrosis and protects against muscle weakness after massive rotator cuff tear. *J Shoulder Elbow Surg*. 2015;24(2):280–287. doi:10.1016/j.jse.2014.06.048
22. Oka S, Matsumoto T, Kubo S, et al. Local administration of low-dose simvastatin-conjugated gelatin hydrogel for tendon-bone healing in anterior cruciate ligament reconstruction. *Tissue Eng Part A*. 2013;19(9–10):1233–1243. doi:10.1089/ten.TEA.2012.0325
23. Tucker JJ, Soslowsky LJ. Effect of simvastatin on rat supraspinatus tendon mechanical and histological properties in a diet-induced hypercholesterolemia model. *J Orthop Res*. 2016;34(11):2009–2015. doi:10.1002/jor.23225
24. de Oliveira LP, Vieira CP, Da re guerra F, De almeida Mdos S, Pimentel ER. Statins induce biochemical Changes in the Achilles tendon after chronic treatment. *Toxicology*. 2013;311(3):162–168. doi:10.1016/j.tox.2013.06.010
25. Eliasson P, Svensson RB, Giannopoulos A, et al. Simvastatin and atorvastatin reduce the mechanical properties of tendon constructs in vitro and introduce catabolic Changes in the gene expression pattern. *PLoS One*. 2017;12(3):e0172797. doi:10.1371/journal.pone.0172797

26. Deren ME, Ehteshami JR, Dines JS, et al. Simvastatin exposure and rotator cuff repair in a rat model. *Orthopedics*. 2017;40(2):e288–e92. doi:10.3928/01477447-20161128-02

27. Jeong C, Kim SE, Shim KS, et al. Exploring the in vivo anti-inflammatory actions of simvastatin-loaded porous microspheres on inflamed tenocytes in a collagenase-induced animal model of Achilles tendinitis. *Int J Mol Sci*. 2018;19(3):820. doi:10.3390/ijms19030820

28. Kaleagasioglu F, Olcay E, Olgac V. Statin-induced calcific Achilles tendinopathy in rats: comparison of biomechanical and histopathological effects of simvastatin, atorvastatin and rosuvastatin. *Knee Surg Sports Traumatol Arthrosc*. 2017;25(6):1884–1891. doi:10.1007/s00167-015-3728-z

29. Liu KS, Kao CW, Tseng YY, et al. Assessment of antimicrobial agents, analgesics, and epidermal growth factors-embedded anti-adhesive poly (lactic-co-glycolic acid) nanofibrous membranes: in vitro and in vivo studies. *Int J Nanomedicine*. 2021;16:4471–4480. doi:10.2147/IJN.S318083

30. Abdel Hakiem AF, Mohamed NA, Ali HRH. FTIR spectroscopic study of two isostructural statins: simvastatin and Lovastatin as authentic and in pharmaceuticals. *Spectrochim Acta A Mol Biomol Spectrosc*. 2021;261:120045. doi:10.1016/j.saa.2021.120045

31. Singh H, Philip B, Pathak K. Preparation, characterization and pharmacodynamic evaluation of fused dispersions of simvastatin using PEO-PPO block copolymer. *Iran J Pharm Res*. 2012;11(2):433–445.

32. Pedersen TR, Tobert JA. Simvastatin: a review. *Expert Opin Pharmacother*. 2004;5(12):2583–2596. doi:10.1517/14656566.5.12.2583

33. Weber C, Erl W, Weber KS, Weber PC. HMG-CoA reductase inhibitors decrease CD11b expression and CD11b-dependent adhesion of monocytes to endothelium and reduce increased adhesiveness of monocytes isolated from patients with hypercholesterolemia. *J Am Coll Cardiol*. 1997;30 (5):1212–1217. doi:10.1016/s0735-1097(97)00324-0

34. Buchwald H, Campos CT, Boen JR, Nguyen PA, Williams SE. Disease-free intervals after partial ileal bypass in patients with coronary heart disease and hypercholesterolemia: report from the Program on the Surgical Control of the Hyperlipidemias (POSCH). *J Am Coll Cardiol*. 1995;26 (2):351–357. doi:10.1016/0735-1097(95)80006-3

35. Naito Y, Terukina T, Galli S, et al. The effect of simvastatin-loaded polymeric microspheres in a critical size bone defect in the rabbit calvaria. *Int J Pharm*. 2014;461(1–2):157–162. doi:10.1016/j.ijpharm.2013.11.046

36. Li X, Liu X, Ni S, Liu Y, Sun H, Lin Q. Enhanced osteogenic healing process of rat tooth sockets using a novel simvastatin-loaded injectable microsphere-hydrogel system. *J Craniomaxillofac Surg*. 2019;47(7):1147–1154. doi:10.1016/j.jcms.2019.04.011

37. Esenkaya I, Sakarya B, Unay K, Elmali N, Aydin NE. The influence of atorvastatin on tendon healing: an experimental study on rabbits. *Orthopedics*. 2010;33(6):398. doi:10.3928/01477447-20100429-06

38. Contractor T, Beri A, Gardiner JC, Tang X, Dwamena FC. Is statin use associated with tendon rupture? A population-based retrospective cohort analysis. *Am J Ther*. 2015;22(5):377–381. doi:10.1097/MJT.0000000000000039

39. Beri A, Dwamena FC, Dwamena BA. Association between statin therapy and tendon rupture: a case-control study. *J Cardiovasc Pharmacol*. 2009;53(5):401–404. doi:10.1097/FJC.0b013e3181a0ce8b

40. Lin TT, Lin CH, Chang CL, Chi CH, Chang ST, Sheu WH. The effect of diabetes, hyperlipidemia, and statins on the development of rotator cuff disease: a nationwide, 11-year, longitudinal, population-based follow-up study. *Am J Sports Med*. 2015;43(9):2126–2132. doi:10.1177/0363546515588173

41. Hoffman KB, Kraus C, Dimbil M, Golomb BA. A survey of the FDA's AERS database regarding muscle and tendon adverse events linked to the statin drug class. *PLoS One*. 2012;7(8):e42866. doi:10.1371/journal.pone.0042866

42. de Oliveira LP, Vieira CP, Guerra FD, Almeida MS, Pimentel ER. Structural and biomechanical changes in the Achilles tendon after chronic treatment with statins. *Food Chem Toxicol*. 2015;77:50–57. doi:10.1016/j.fct.2014.12.014

43. Marie I, Delafenetre H, Massy N, Thuillez C, Noblet C; Network of the French Pharmacovigilance Centres. Tendinous disorders attributed to statins: a study on ninety-six spontaneous reports in the period 1990–2005 and review of the literature. *Arthritis Rheum*. 2008;59(3):367–372. doi:10.1002/art.23309

44. Makadia HK, Siegel SJ. Poly lactic-co-glycolic acid (PLGA) as biodegradable controlled drug delivery carrier. *Polymers*. 2011;3(3):1377–1397. doi:10.3390/polym3031377

45. Kapoor DN, Bhatia A, Kaur R, Sharma R, Kaur G, Dhawan S. PLGA: a unique polymer for drug delivery. *Ther Deliv*. 2015;6(1):41–58. doi:10.4155/tde.14.91

46. Xue J, Wu T, Dai Y, Xia Y. Electrospinning and electrospun nanofibers: methods, materials, and applications. *Chem Rev*. 2019;119(8):5298–5415. doi:10.1021/acs.chemrev.8b00593

47. Islam MS, Ang BC, Andriyana A, Afifi AM. A review on fabrication of nanofibers via electrospinning and their applications. *SN Appl Sci*. 2019;1 (10):1248. doi:10.1007/s42452-019-1288-4

48. Hines DJ, Kaplan DL. Poly(lactic-co-glycolic) acid-controlled-release systems: experimental and modeling insights. *Crit Rev Ther Drug Carrier Syst*. 2013;30(3):257–276. doi:10.1615/critrevtherdrugcarriersyst.2013006475

49. Xu Y, Shi G, Tang J, et al. ECM-inspired micro/nanofibers for modulating cell function and tissue generation. *Sci Adv*. 2020;6(48):eabc2036. doi:10.1126/sciadv.abc2036

50. Anjum F, Agabalyan NA, Sparks HD, Rosin NL, Kallos MS, Biernaskie J. Biocomposite nanofiber matrices to support ECM remodeling by human dermal progenitors and enhanced wound closure. *Sci Rep*. 2017;7(1):10291. doi:10.1038/s41598-017-10735-x

51. Nemati S, Kim SJ, Shin YM, Shin H. Current progress in application of polymeric nanofibers to tissue engineering. *Nano Converg*. 2019;6(1):36. doi:10.1186/s40580-019-0209-y